CHAPTER 5: Evidence for an Extended Hydrogen Bond Network in the Binding Site of the Nicotinic Receptor: Concerning the Role of the Vicinal Disulfide of the α1 Subunit*

5.1 ABSTRACT

The defining feature of the α subunits of the family of nicotinic acetylcholine receptors is a vicinal disulfide between C192 and C193. While this structure has played a pivotal role in a number of pioneering studies of nicotinic receptors, its functional role in native receptors remains uncertain. Using mutant cycle analysis and unnatural residue mutagenesis, including backbone mutagenesis of the peptide bond of the vicinal disulfide, we have established the presence of a network of hydrogen bonds that extends from that peptide NH, across a β turn to another backbone hydrogen bond, and then across the subunit interface to the side chain of a functionally important Asp residue in the non-α subunit. We propose that the role of the vicinal disulfide is to distort the β turn and thereby properly position a backbone NH for intersubunit hydrogen bonding to the key Asp.

5.2 INTRODUCTION

Nicotinic acetylcholine receptors (nAChRs) are neurotransmitter-gated ion channels that mediate rapid synaptic transmission throughout the central and peripheral nervous

---

* *This work was done in collaboration with Kristin Rule Gleitsman and is adapted from:* Blum, A. P.; Gleitsman, K. R.; Lester, H. A.; Dougherty, D. A., Evidence for an extended hydrogen bond network in the binding site of the nicotinic receptor: concerning the role of the vicinal disulfide of the α1 subunit. *The Journal of Biological Chemistry* **2011**, *286*, (37), 32251-58.

systems.[1-3] The nAChR family members are also the prototypes of a large class of channels termed Cys-loop (or pentameric) receptors, which are essential for learning, memory, and sensory perception, and are implicated in numerous neurological disorders, including Alzheimer's disease, Parkinson's disease, and schizophrenia.[4, 5] Of the seventeen genes that code for subunits of the nAChR, ten produce α subunits. The α subunits of nAChRs typically contain the principal component of the agonist binding site and are distinguished by a unique vicinal disulfide at the agonist binding site formed by residues canonically labeled as C192 and C193. As shown in **Figure 5.1**, the vicinal disulfide produces an eight-membered ring that contains an amide and a disulfide, two functionalities with distinct conformational properties.

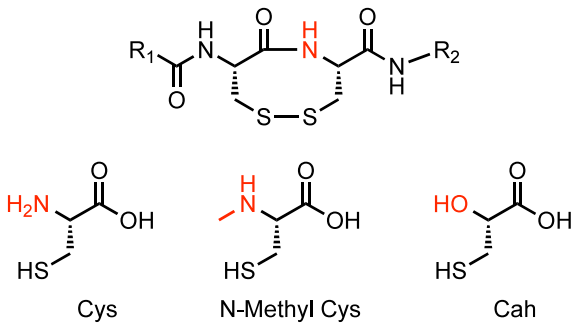

Figure 5.1. Vicinal disulfide structure. For model calculations of CH_3CO-[Cys-Cys]-NH_2, R_1 = CH_3 and R_2 = H. Also shown are the unnatural amino acids (*N*-Methyl Cys and α-hydroxy cysteine, Cah) used in this study.

In the 1960s, reduction of this disulfide in the *Electrophorus* electroplax led to the realization that the nAChR, long defined as controlling the membrane's ion conductance, is a protein.[6-8] That this disulfide can be more easily reduced than a typical protein disulfide was later rationalized by the finding that the disulfide is vicinal and therefore embedded in a strained ring.[9, 10] The vicinal disulfide has been included and discussed in

many classic studies in early nAChR research owing to its susceptibility to reduction, and proximity to the agonist binding site.[6, 7, 11-16]

Nevertheless, the precise role of the vicinal disulfide in nAChR function is not established. Early studies[17] seemed to indicate that reduction of this disulfide rendered the receptor non-functional (but see below). Computational, NMR, and crystallographic studies of model vicinal disulfides have probed the multiple conformational possibilities of this unique structural unit.[18-22] The *trans* conformation that is overwhelmingly preferred for backbone amides is expected to be disfavored in the context of an eight-membered ring, allowing for an energetically accessible *cis* backbone conformation. Also, a gauche conformation is strongly preferred about the S-S disulfide bond (C-S-S-C dihedral angle ~90°). In the context of the ring formed by the vicinal disulfide, the gauche(+) and gauche(−) forms produce energetically distinct (diastereomeric) structures. The combined backbone and disulfide conformational combinations give rise to four distinct conformers for the vicinal disulfide ring.

While the sulfurs of the disulfide can contact small molecules that bind to the acetylcholine binding protein (AChBP),[23, 24] a very useful model of the nAChR binding site, any noncovalent interactions of this sort are expected to be quite weak. Instead, we and others have speculated on a role in receptor gating involving *cis*-*trans* isomerization of the amide and/or gauche(+)/gauche(−) interconversion of the disulfide.[10, 18, 19, 21, 22] Conventional mutagenesis studies are expected to produce severely impaired receptors, and so it has been challenging to design unambiguous probes of disulfide function.

Here we use subtle structural variations enabled by unnatural amino acid mutagenesis to evaluate the possible functional role of the vicinal disulfide of nAChR α

subunits. We find evidence that the vicinal disulfide contributes to an interesting triad of residues that forms a network of hydrogen bonds that spans the interface between two subunits and impacts receptor function.

5.3 RESULTS

5.3.1 Conformational Analysis and Experimental Design

As noted above, both the disulfide and the amide functionalities have two distinct conformations. In the computational studies described below the gauche(+) and gauche(−) forms of the disulfide are very similar in energy, and seem unlikely to play a strong discriminating role. Our work has emphasized the gauche(−), as this is the conformation seen in AChBP crystal structures.

For the amide unit, the issue is *cis*-*trans* isomerization. In a typical protein a backbone amide shows a strong preference for the *trans* conformation (if proline is not involved). However, incorporation into an eight-membered ring is expected to favor the *cis* form. This expectation derives from studies of the conformational preferences of small molecules. For example, in cyclooctene the *trans* form is substantially strained, and the *cis* form is preferred. *Ab initio* calculations we have performed show that an amide in an eight-membered alkane ring also shows a preference for *cis*; at the HF-6-31G** level of theory, *N*-methylacetamide shows a 2.5 kcal/mol preference for *trans*, while the cyclic amide shows a 5.4 kcal/mol preference for *cis*.

More sophisticated calculations at the B3LYP/6-311++G(d,p) level of theory on a model tripeptide (CH_3CO-[Cys-Cys]-NH_2, **Figure 5.1**) for the nAChR vicinal disulfide likewise show an energetic preference for the *cis* amide, by 3.4 kcal/mol. This is not a large energy difference, and, indeed, both *cis* and *trans* forms have been seen in crystal

structures of molecules that contain a vicinal disulfide.[25, 26] We and others have for some time speculated that perhaps *cis*-*trans* isomerization of the C192-C193 backbone may play a role in gating of nAChRs. This structural change could then easily be imagined to propagate along the protein backbone and perhaps initiate the "conformational wave"[27] that leads to gating.

To test this model, we sought modifications to the vicinal disulfide that would alter the innate *cis*-*trans* bias of the system. For example, it is well known[28] that esters have a stronger *trans* preference than amides; methyl acetate prefers *trans* by 8.0 kcal/mol compared to the 2.5 kcal/mol noted for *N*-methylacetamide above. It is also well established that *N*-methylation reduces the innate *trans* preference of a backbone amide in peptides and proteins.[29, 30] Thus, we considered the strategy of modifying the amide linkage of the vicinal disulfide. If *cis*-*trans* isomerization of this unit plays a role in receptor function, then the ester and *N*-methyl modifications should have opposite effects.

To test this prediction *in silico*, we performed comparable B3LYP/6-311++G(d,p) calculations on the ester and *N*-methyl amide analogs of the vicinal disulfide model discussed above. The results are consistent with expectation based on the conformational preferences of small molecules discussed above. Compared to the natural backbone (an amide), which favors the *cis* by 3.4 kcal/mol, the ester favors the *trans* by 1.4 kcal/mol. *N*-methylation increases the *cis* preference of the parent (the amide backbone) to 9.3 kcal/mol, consistent with experimental studies on a similar system reported by Hondal.[22]

It is difficult to apply these data to nAChR function in a quantitative way; calculations were performed on model tripeptides and depsipeptides in the gas phase, not

on a ~2.5MDa pentameric, polytropic receptor protein in a cell membrane. However, the predictions of the calculations are clear. If *cis-trans* isomerization of the vicinal disulfide amide is functionally important, the two modifications considered – backbone ester incorporation and amide *N*-methylation – should have opposite effects on receptor function.

Both modifications can be site-specifically introduced into the nAChR using the *in vivo* nonsense suppression methodology that has been developed in our labs over the past 20 years.[31, 32] We thus set out to prepare and characterize the appropriate mutant receptors as a test of the computational modeling.

5.3.2 Mutagenesis Studies

Initial control experiments involving the vicinal disulfide clarified the effect of eliminating this structure. We found that we could introduce Ala or Ser at C192 or C193 of the wild-type muscle subtype receptor and obtain functional receptors. The EC_{50} value shifts ~8−40 fold (**Table 5.1**), and current sizes comparable to those for the wild-type receptor are seen. We repeated these studies in three other subtypes of the nAChR – the neuronal receptors α4β2, α4β4 and α7 – and saw similar effects, but with generally larger shifts in EC_{50} (~20 to 200-fold, **Table 5.2**).

Table 5.1. EC_{50}, Hill coefficient (± standard error of the mean) and ΔG° values for mutations made to $\alpha 1_2\beta 1\gamma\delta$.

Mutation	EC_{50} (μM)	Hill	ΔG° (kcal/mol)
α1β1γδ	18 ± 0.2	1.4 ± 0.01	-
α1(C192A)β1γδ	660 ± 20	1.3 ± 0.05	2.1
α1(C192S)β1γδ	520 ± 20	1.5 ± 0.08	2.0
α1(C193A)β1γδ	140 ± 3	1.2 ± 0.02	1.2
α1(C193S)β1γδ	150 ± 7	1.4 ± 0.07	1.3
α1β1(L9'S)γδ	0.61 ± 0.04	1.4 ± 0.1	-
α1(S191A)β1(L9'S)γδ	0.31 ± 0.02	1.1 ± 0.05	-
α1(S191A/C193A)β1(L9'S)γδ	5.2 ± 0.4	1.0 ± 0.07	1.7
α1(S191A/C193S)β1(L9'S)γδ	9.5 ± 0.7	0.96 ± 0.06	2.0
α1(S191A/C193Cah)β1(L9'S)γδ	49 ± 4	0.80 ± 0.03	3.0
α1(S191A/C193*N*-Me-Cys)β1(L9'S)γδ	39 ± 2	0.88 ± 0.04	2.9
α1(S191Aah)β1(L9'S)γδ	31 ± 3	1.1 ± 0.09	2.7
α1(S191A)β1(L9'S)γ(D174N)δ(D180N)	160 ± 7	1.3 ± 0.06	3.7

Table 5.2. EC_{50}, Hill coefficient (± standard error of the mean) and ΔG° values for each mutation made to the vicinal disulfide in neuronal receptors, α4β4, α7 and α4β2. n.d. = value not determined due to low current sizes for the indicated mutations. The stoichiometry of the α4β2 ($\alpha 4_2\beta 2_3$) protein was verified as described previously.[33] The stoichiometry of α4β4 is assumed to be $\alpha 4_2\beta 4_3$ based on injection ratios of each subunit as discussed elsewhere.[34]

Mutation	EC_{50} (μM)	Hill	ΔG° (kcal/mol)
human α4β4			
α4β4	15 ± 2	1.2 ± 0.1	-
α4(C197A)β4	180 ± 6	1.5 ± 0.05	1.5
α4(C197S)β4	n.d.	-	-
α4(C198A)β4	160 ± 10	1.3 ± 0.1	1.4
α4(C198S)β4	280 ± 10	1.7 ± 0.1	1.7
rat α7(T6'S)			
α7(T6'S)	94 ± 2	2.2 ± 0.1	-
α7(T6'S/C189A)	7300 ± 600	2.1 ± 0.3	2.6
α7(T6'S/C189S)	n.d	-	-
α7(T6'S/C190A)	4100 ± 300	2.3 ± 0.3	2.2
α7(T6'S/C190S)	n.d.	-	-
rat $\alpha 4(L9'A)_2\beta 2_3$			
α4(L9'A)β2	0.36 ± 0.02	1.3 ± 0.07	-
α4(L9'A/C197A)β2	80 ± 10	0.87 ± 0.07	3.2
α4(L9'A/C197S)β2	69 ± 10	0.91 ± 0.1	3.1
α4(L9'A/C198A)β2	47 ± 4	1.1 ± 0.09	2.9
α4(L9'A/C198S)β2	84 ± 10	1.1 ± 0.1	3.2

In 1985, Mishina *et al.* reported that C192S and C193S mutants of *Torpedo* nAChR, a close paralog of the muscle nAChR, were unresponsive to high concentrations of ACh, but did bind α-bungarotoxin.[17] These findings suggested that mutation of either residue results in a receptor that is properly folded, but does not function. However, our

present finding that the nAChR can be activated even in the presence of mutated 192 and 193 side chains indicates that the vicinal disulfide linkage increases the efficiency of receptor function, but is not absolutely required.

In these studies we are reporting EC_{50} values, a functional measure that includes contributions from both ligand binding and receptor gating. For the residues emphasized here, there is no evidence that C192 and C193 interact strongly and directly with agonists, and so we anticipate that mutations primarily impact receptor gating, although we cannot prove that unambiguously. In upcoming discussion, we will be describing the results of mutant cycle analysis studies. It is standard practice in that field to convert coupling interactions (nonadditivity) to free energies ($\Delta\Delta G°$).[35, 36] In view of this, and solely for the purpose of discussion, we will put all changes in EC_{50} values on a similar energy scale: $\Delta G° = RTln[EC_{50}(mutant)/EC_{50}(wild\ type)]$.

Before launching detailed nonsense suppression experiments with *N*-methyl Cys and Cah (cysteine, α-hydroxy), we considered several conditions and nAChR subtypes, including the muscle receptor $\alpha1_2\beta1\gamma\delta$ and the neuronal subtypes α4β2, α4β4 and α7. We chose to focus on the muscle subtype for the following reasons. The muscle subtype is, in general, the most studied nAChR, and it is also the receptor that gave the highest currents for nonsense suppression experiments with *N*-methyl Cys and Cah. In addition, it has a defined stoichiometry, a substantial advantage over the α4β2 and α4β4 receptors (which each have two possible subunit stoichiometries). It also required considerably lower agonist concentrations than those needed for experiments with α7.

For our nonsense suppression experiments in $\alpha1_2\beta1\gamma\delta$, we used the well-documented leucine to serine mutation at the 9' position in the M2 region of nAChR.

This mutation renders the nAChR ~40-times more sensitive to agonists, as judged by the decrease in EC_{50}.[37, 38] The 9' position lies some 60 Å from the agonist binding site and from the vicinal disulfide studied here, and therefore it does not directly affect the C192-C193 region, but instead affects receptor gating. This change favors the open state of the channel once an agonist molecule has bound, also increasing the efficacy of some agonists.

We also introduced a mutation in the α1 subunit, S191A, of all mutant proteins used in double mutant cycle analyses as this mutant promoted more reliable current sizes for nonsense suppression experiments with α-hydroxy acids at position 191, experiments that will be discussed in greater detail below. We showed previously[39] that the S191A mutation has a minor effect on receptor function (see also **Table 5.1)** and that the incorporation of Aah (alanine, α-hydroxy) or Sah (serine, α-hydroxy) at S191 results in the same EC_{50} shift.

In the crucial experiments involving alteration of the backbone of the C192-C192 unit, we find that replacement of C193, whose backbone is within the eight-membered ring formed by the vicinal disulfide, with either *N*-methyl Cys or Cah produces *similar* results. Both mutations are loss-of-function, and their impacts are comparable in magnitude, with a ΔG° value of ~3 kcal/mol. These are relatively large effects for such subtle mutations (larger than the Cys-to-Ala mutations), suggesting an important functional role for the backbone of C193. These results are not consistent with a functional role for *cis-trans* isomerization, which predicts opposite effects for the two modifications.

While differing in their anticipated impact on *cis-trans* isomerization, the two backbone mutations are similar in another regard: both ablate the hydrogen bond-donating ability associated with the NH of the parent amide. An inspection of AChBP structures reveals a potential acceptor for such a hydrogen bond donor: the carbonyl of residue Y190, a conserved member of the agonist binding site. This hydrogen bond is generally present in AChBP structures, and it defines a distorted Type I β turn, with Y190, S191, C192, and C193 being residues *i* to *i+3*, respectively (**Figure 5.2**).

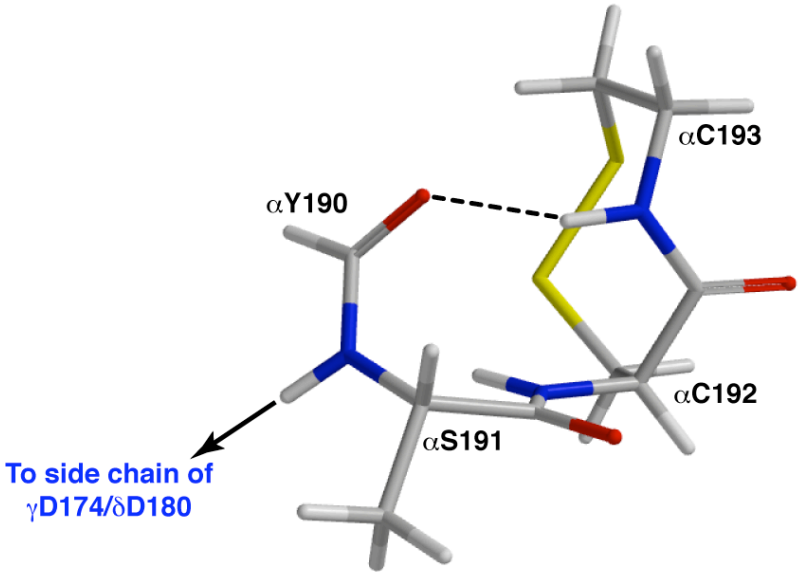

Figure 5.2. The β turn found in AChBP structures. Structure is from pdb file 1UV6 [24] and was modified to contain an Ala at S191.[24] The side chain of Tyr190 is truncated (replaced with a hydrogen) for simplicity.

The inclusion of S191 in the β turn suggested a more complex interaction than just a simple hydrogen bond. Previous work from our labs[39] strongly supported a model in which the backbone NH of S191 makes an *intersubunit* hydrogen bond to the side chain of a critical Asp in the γ/δ subunits (γD174/δD180; δD174 is in the δ sequence WIIIDPEGF and γD180 is in the γ sequence WIFIDPEAF). This hydrogen bond contributes to ion channel gating. In that study, we removed the critical NH by preparing

the mutant S191Sah or S191Aah, producing one of the largest perturbations ever observed in our labs for the introduction of a backbone ester. A double mutant cycle analysis combining S191Sah and γD174N/δD180N provided strong functional evidence for an interaction, with a coupling energy ΔΔG° = 2.7 kcal/mol. However, many studies have shown that a backbone ester mutation not only removes a backbone NH that can donate a hydrogen bond, it also weakens the hydrogen bond-accepting ability of the associated *i-1* carbonyl.[40-45] For S191 the *i-1* carbonyl comes from Y190, the carbonyl implicated in the hydrogen bond of the β turn discussed above. Could the S191Sah effect be so large because it both deletes the hydrogen bond to γD174/δD180 and weakens an important β turn hydrogen bond?

We have now found support for the β turn hydrogen bond. A mutant cycle analysis (**Figure 5.3A**) combining S191Aah and C193(*N*-methyl Cys) shows a strong coupling energy, with ΔΔG° = 2.7 kcal/mol (**Table 5.3**). This finding supports the existence of a novel, 3-residue, hydrogen bond network, in which the NH of C193 hydrogen bonds to the carbonyl of the peptide bond between Y190 and S191. In addition, the NH of the Y190-S191 peptide bond hydrogen bonds to the side chain of γD174/δD180 (**Figure 5.3**).

Table 5.3. EC_{50}, Hill coefficient (± standard error of the mean) and ΔΔG° values for double mutations made to $\alpha 1_2\beta 1\gamma\delta$.

Double Mutation	EC_{50} (μM)	Hill	ΔΔG° (kcal/mol)
α1(S191Aah/C193A)β1(L9'S)γδ	97 ± 10	0.76 ± 0.04	0.99
α1(S191Aah/C193S)β1(L9'S)γδ	100 ± 7	0.93 ± 0.05	1.3
α1(S191Aah/C193*N*-Me-Cys)β1(L9'S)γδ	39 ± 4	0.70 ± 0.03	2.7
α1(S191Aah)β1(L9'S)γ(D174N)δ(D180N)	140 ± 10	1.7 ± 0.2	2.8
α1(S191A/C193A)β1(L9'S)γ(D174N)δ(D180N)	600 ± 20	1.5 ± 0.07	0.8
α1(S191A/C193S)β1(L9'S)γ(D174N)δ(D180N)	780 ± 20	1.6 ± 0.06	1.1
α1(S191A/C193Cah)β1(L9'S)γ(D174N)δ(D180N)	800 ± 40	1.5 ± 0.05	2
α1(S191A/C193*N*-Me-Cys)β1(L9'S)γ(D174N)δ(D180N)	500 ± 20	1.5 ± 0.07	2.2

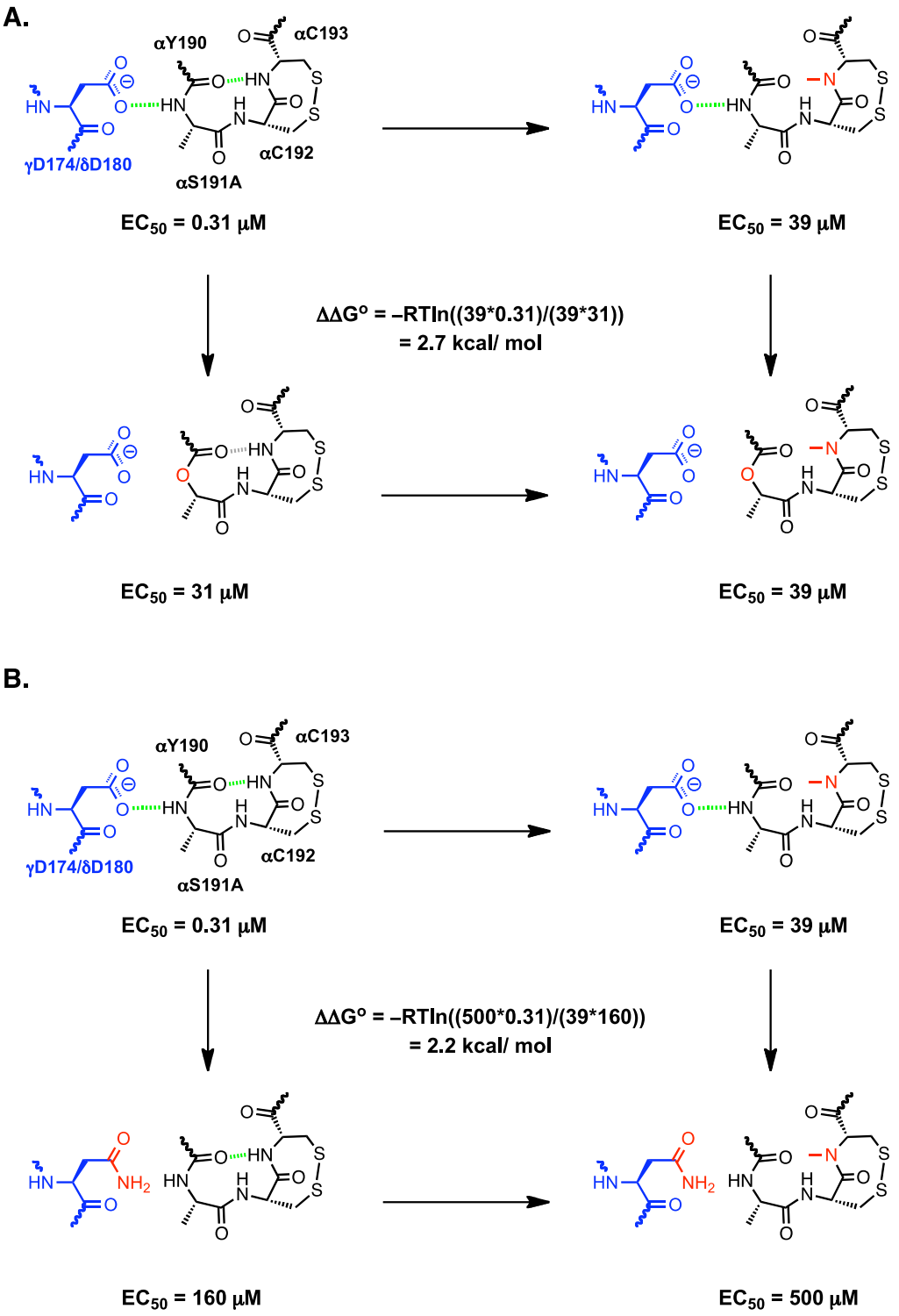

Figure 5.3. Double mutant cycle analyses. (A) Coupling between backbone mutations at αS191 and αC193. Note that introduction of the α-hydroxy acid at S191 attenuates the hydrogen bond acceptor for the hydrogen bond with C193 and removes the hydrogen bond donor for the hydrogen bond to γD174/δD180. (B) Long-range coupling between a backbone mutation at αS191 and a side chain mutation at γD174/δD180.

If this hydrogen bonding network exists, energetic coupling between the NH of C193 and the side chain of γD174/δD180 is expected. Indeed, we find strong coupling energies between the γD174N/δD180N mutation and either C193(*N*-methyl Cys) or C193Cah, with ΔΔG° values of 2.0 and 2.2 kcal/mol (**Table 5.3**, **Figure 5.3B**). The magnitude of this interaction is quite significant when one considers the linkage is from a residue in the α subunit, through a second residue in the α subunit, and then across the subunit interface to a residue in the γ/δ subunit.

These results suggest a key role for the peptide bond of the C192-C193 unit. In support of this view, mutations that remove the disulfide but keep the peptide bond are much less impactful. Mutant cycles that link C193A to the backbone NH of S191 or to γD174N/δD180N produce ΔΔG° coupling energies of 0.99 and 0.80 kcal/mol, respectively, clearly smaller than what is seen with backbone mutations.

A three-dimensional mutant cycle analysis (**Figure 5.4**) was also performed using the triple mutant α1C193A/α1S191Aah/(γD174N/δD180N) in which each member of the triad is mutated. This triple mutation gave an EC_{50} of 480 μM, smaller than what was seen for the double mutant α1C193A/(γD174N/δD180N). Note that we were unable to obtain a dose-response relation for a triple mutant involving a backbone mutation at C193 due to small current sizes.

Figure 5.4. Three-dimensional mutant cycle analysis with the triple mutant, α1C193A/α1S191Aah/(γD174N/δD180N).

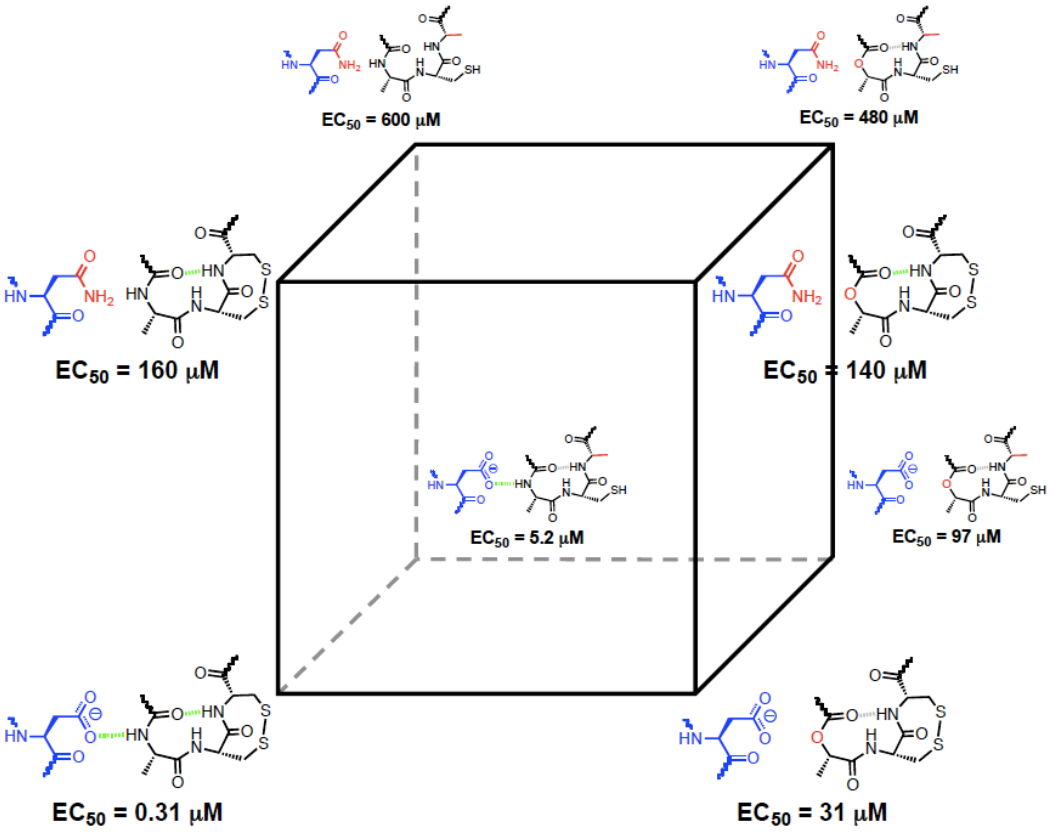

Table 5.4. Coupling energies for each face of the three-dimensional mutant cycle. ΔΔΔ°G = ΔΔG° front face – ΔΔG° back face = ΔΔG° left face – ΔΔG° right face = ΔΔG° bottom face – ΔΔG° top face.

Face	ΔΔG° (kcal/mol)
Front	2.8
Back	1.9
Left	0.89
Right	−0.054
Bottom	0.99
Top	0.053
ΔΔΔG°	**~0.9**

Multidimensional mutant cycle analysis is used to measure higher-order cooperativity between intramolecular or intermolecular interactions in proteins.[35, 46-48] Subtraction of the coupling energies (ΔΔG° values) from parallel faces of the three-

dimensional mutant cycle (**Table 5.4**) gives the ΔΔΔG° of the system, which is essentially an approximation of the extent that one interaction activates the other interaction[35] (*e.g.*, how much the hydrogen bond between of the β turn activates the intersubunit hydrogen bond). The ΔΔΔG° of this system is relatively large, ~0.9 kcal/mol, suggesting that each interaction in the hydrogen bond network is strengthened when the other interaction is present. This is consistent with our model, given that the two hydrogen bonds should reinforce one another – the β turn hydrogen bond should make the S191 backbone NH a better hydrogen bond donor, and the intersubunit hydrogen bond should make the Y190 CO a better hydrogen bond acceptor by withdrawing or adding electron density through the amide bond, respectively.

5.4 DISCUSSION

The present work began as an effort to evaluate a possible role for *cis-trans* isomerization of the C192-C193 peptide bond embedded in the unusual vicinal disulfide of the α subunits of nAChRs. Our data do not support such a transition, but instead reveal an extended network of hydrogen bonds that appears to play a significant role in receptor function. In this network, the backbone NH of C193 hydrogen bonds to the backbone carbonyl of Y190. The Y190 carbonyl is, in turn, connected to the NH of S191, which hydrogen bonds across the subunit interface to the side chain of γD174/δD180. The model is strongly supported by long-range double mutant cycle analysis that links the γD174N/δD180N mutation to C193 backbone mutations. Removing the NH of C193 either by ester incorporation or *N*-methylation produces the same effect: a coupling energy ΔΔG° of 2.0-2.2 kcal/mol to the D-to-N mutations.

The β turn hydrogen bond between the carbonyl of Y190 and the NH of C193 was suggested by AChBP structures.[23, 24] Note, however, that the second hydrogen bond of the triad – that between the NH of S191 and the side chain of γD174/δD180 – is not present in AChBPs and represents a significant difference between the actual nAChRs and the model AChBP systems. In fact, in crystal structures of AChBP, the loop F residue that corresponds to γD174/δD180 is far from the adjacent subunit's C loop, and in the cryoelectron microscopy structures of *Torpedo* nAChR, the residue is over 15 Å from the C loop.[49, 50]

Given these data, what then is the functional role of the C192-C193 vicinal disulfide of nAChR α subunits? Here we present a speculative model. An early mutagenesis study of the *Torpedo* nAChR indicated that both the C192S and C193S mutants were unresponsive to high concentrations of ACh.[17] However DTT reduction of the vicinal disulfide produced only partial diminution of receptor function,[6] and alkylation of one of these cysteines by bromo-acetylcholine[8] or QBr [16] reinstates partial function despite the absence of the vicinal disulfide. Here we also find that in mouse muscle and several neuronal nAChRs, conventional mutations at C192/C193, while certainly loss-of-function, do produce functional receptors. In the present case, C192A and C193A are both loss-of-function, but the magnitudes of the effects (2.0 and 1.7 kcal/mol with the α1S191A background mutation) are *less* than what is seen with the backbone mutations (2.9 and 3.0 kcal/mol), for which the disulfide linkage is intact.

We propose that the role of the vicinal disulfide is to shape the structure of the β turn between Y190 and C193. The resultant distorted β turn may then help position the backbone NH of S191 for formation of the second hydrogen bond. Such a model is

supported by the observation that backbone mutations at C193 are strongly loss-of-function, suggesting that backbone positioning in this β turn is critical for receptor function.

We noted above that the β turn seen in AChBP structures is substantially distorted from idealized dihedral angle values for a Type I β turn. Quantum mechanical calculations (details available in the Supplemental Material of Blum *et al*.[51]) establish that reducing the disulfide does indeed allow the β turn to relax toward a more typical geometry. This structural change impacts the energetic strength of the β turn hydrogen bond only modestly (0.3 to 0.4 kcal/mol), but it does alter the positioning of the peptide linkage between Y190 and S191. Thus, we propose that the essential consequence of the distortion of the β turn induced by the disulfide is not the energetic weakening of the β turn hydrogen bond, but rather the positioning of S191 in an orientation that is favorable for interaction with γD174/δD180.

Our gating model is thus as follows. In the closed state of the receptor, the β turn hydrogen bond is formed, but the intersubunit hydrogen bond (S191 to γD174/δD180) is not (consistent with the AChBP crystal structures). The β turn hydrogen bond is essential to proper formation of the agonist binding site (recall that Y190 is residue C1 of the highly conserved cluster of aromatic amino acids that delineate the agonist binding site). Activation involves formation of the intersubunit hydrogen bond, an event that is facilitated by proper positioning of the backbone NH of S191 by the vicinal disulfide and the β turn hydrogen bond. The two hydrogen bonds should be mutually reinforcing, making the amide a stronger hydrogen bond acceptor and donor, which is reflected in the three-dimensional mutant cycle analysis done with the α1C193A/α1S191Aah/

(γD174N/δD180N) triple mutant where it was found that each interaction was strengthened by 0.9 kcal/mol when the other interaction is present. Thus, in our model the driving force for movement of the F loop (containing γD174/δD180) is the formation of a network of hydrogen bonds. As discussed elsewhere,[39] this structural change at the subunit interface then contributes to an early phase of the conformational wave of receptor gating.

Note that our conventional mutations of C192 and C193, both of which are loss-of-function, are consistent with this model. The C192A and C193A mutants remove the disulfide and allow the β turn to relax to a more typical conformation (mirrored in the calculations). With the β turn relaxed, the backbone NH of S191 is not positioned optimally to form a hydrogen bond with γD174/δD180, resulting in a loss of receptor function. The critical role of the peptide bond is further supported by our observation that disruption of the vicinal disulfide (C193A) perturbs the hydrogen bond network in a much more subtle manner than removal of the hydrogen bond donor of C193. Other Cys-loop receptors lack the vicinal disulfide of the nAChR α subunit, and it will be interesting to see if the β turn and intersubunit hydrogen bond survive in a different environment.

The vicinal disulfide has a unique historical connection to γD174/δD180. Czajkowski and Karlin linked the reduced cysteine side chain at position α193 to γD174/δD180 with a 9 Å cross-linker.[11, 12, 14, 52] Mutation of the aspartate resulted in a large loss of receptor function, leading to the suggestion that the negative charge of the aspartate side chain interacts directly with the positive charge of the agonist. Subsequent mutagenesis studies showed that the positive charge of agonists makes a cation-π interaction to a conserved tryptophan[33, 53] and not a direct interaction with the aspartate.

Crystallographic studies of AChBP supported the cation-π interaction and revealed that γD174/δD180 is positioned far from the agonist binding site.[24] Single channel studies from the early 2000s suggested that the residue was important for channel gating (and not binding),[54, 55] however a role for the aspartate was only recently discovered. In 2008 we reported that γD174/δD180 is a member of an important intersubunit hydrogen bond linking the F and C loops and contributing to channel gating.[39] We now report an additional, larger group of hydrogen bonds once again linking the vicinal disulfide to this important residue.

In summary, our mutagenesis studies unambiguously establish, through mutant cycle analysis, a hydrogen bonding network, beginning at the backbone NH of the C192-C193 disulfide, through the backbone amide linkage between Y190-S191, and across the subunit interface to the side chain of γD174/δD180. Based on this, we present a speculative model in which the transition of the receptor from the closed to the open state involves formation of a network of tandem hydrogen bonds. In this model, the vicinal disulfide of the α subunit distorts the C loop β-turn in order to better position the backbone NH of S191 for optimal formation of an intersubunit hydrogen bond.

5.5 EXPERIMENTAL SECTION

Chemical synthesis. Cysteine analogs were prepared as 2-nitrobenzyl (NB) protected thiols. The 2-nitrobenzyl group was removed via irradiation with ~350 nm UV light prior to injection into *Xenopus* oocytes. A synthesis of nitroveratryl-protected cysteine, needed for control experiments, was described previously.[56] Cyanomethyl esters of *N*-Me-Cys and Cah were appended to the dinucleotide dCA and ligated to tRNA and

introduced to the nAChRs via unnatural amino acid mutagenesis as described previously.[57]

Synthesis of *N*-Me-*N*-NVOC-Cys(SNB)-OCH_2CN. A 20 mL scintillation vial was loaded with 4 mL of methanol and placed over an ice water bath. To this was added 130 mg (5.7 mmol) of Na. The mixture was stirred until the metal dissolved (~20 min). *N*-Me-Cysteine (370 mg, 2.7 mmol), prepared as described previously,[58] was added to the vial and the mixture stirred for 10 minutes. 2-Nitrobenzyl bromide (520 mg, 2.6 mmol) was added in three portions to the stirring solution, turning a clear solution into a cloudy mixture containing a pale yellow precipitate. An hour after the last addition, 20 mL of chilled ether was added. The precipitate was filtered, washed with 10 mL of chilled ether and dried to afford *N*-Me-Cys(S-NB)-OH as a crude, pale yellow solid. 100 mg (0.37 mmol) of this powder was used directly in the next step without further purification. The powder was suspended in 3 mL of water and then an additional 1 mL of dioxane. Na_2CO_3 (59 mg, 0.56 mmol) was added and the mixture was allowed to stir for five minutes prior to the addition of 6-nitroveratryoxycarbonyl chloride (NVOC-chloride) (92 mg, 0.33 mmol) in 4 mL of dioxane. After stirring at room temperature for 48 hours, the solution was diluted with 10 mL of CH_2Cl_2 and 10 mL of water. The organic layer was discarded and the pH of the aqueous layer was decreased to 1 via the addition of 6M HCl. Following extraction with CH_2Cl_2, the new organic layer was dried over Na_2SO_4 and poured over a silica plug. The plug was rinsed with 25 mL of EtOAc and then eluted with 2% AcOH in EtOAc. The yellow eluent was concentrated to reveal *N*-Me-*N*-NVOC-Cys(S-NB)-OH as a pale yellow solid in 84% yield (158 mg, 0.310 mmol). R_f = 0.34 (2% AcOH in EtOAc); ^{1}H NMR (300 MHz, $CDCl_3$, 298 K) δ 7.89 (1H, m), 7.63 (1H,

m), 7.47 (1H, t, *J* = 7.5 Hz), 7.36 (2H, m), 6.89 (1H, d, *J* = 14.1 Hz), 5.50 (2H, m), 4.68 (1H, m), 4.04 (2H, s), 3.86 (6H, s), 2.81 – 3.04 (5H, m); ^{13}C NMR (75 MHz, $CDCl_3$, 298K) δ 177.7, 174.9, 156.4, 153.7, 147.9, 139.3, 133.4, 133.2, 132.1, 128.6, 128.3, 125.6, 109.1, 108.1, 64.7, 58.9, 56.4, 56.4, 33.5, 32.3, 30.9; High-resolution MS analysis (FAB+) *m/z*: calc'd 510.1182, found 510.1180.

N-Me-*N*-NVOC-Cys(S-NB)-OH (58 mg, 0.11 mmol) was added to a 2 mL scintillation vial and suspended in 0.35 mL of chloroacetonitrile (5.5 mmol). Triethylamine (50 mL, 0.33 mmol) was added to the mixture and the resulting solution stirred for 4 hours. The solution was diluted with 15 mL of water and the organic layer was extracted with CH_2Cl_2 (×3), dried over Na_2SO_4 and concentrated to yield a yellow oil. The oil was purified by flash column chromatography on silica gel (50% EtOAC in hexanes) to afford *N*-Me, *N*-NVOC-Cys-(S-NB)-OCH_2CN as a yellow oil in 62% yield (37 mg, 0.067 mmol). R_f = 0.25 (50% EtOAc in hexanes); ^{1}H NMR (300 MHz, $CDCl_3$, 298 K) δ 7.98 (1H, m), 7.70 (1H, m), 7.54 (1H, m), 7.43 (2H, m), 6.95 (1H, d, *J* = 14.1 Hz), 5.55 (2H, m), 4.72 (3H, m), 4.08 (2H, s), 4.00 (3H, s), 3.95 (3H, s), 2.89–3.10 (5H, m); ^{13}C NMR (75 MHz, $CDCl_3$, 298K) δ 168.5, 156.1, 153.7, 148.1, 133.3, 133.3, 133.2, 132.1, 128.7, 128.7, 127.9, 125.6, 109.5, 108.2, 64.9, 59.0, 56.4, 56.4, 49.1, 33.6, 32.7, 31.0; High-resolution MS analysis (FAB+) m/z: calc'd 549.1291, found 549.1302.

Synthesis of HO-Cys(SNB)-OCH_2CN. The synthesis of 2-nitrobenzyl protected α-hydroxy cysteine was based on a protocol reported by Kelly and co-workers.[59] (2-nitrophenyl)methanethiol (400 mg, 3.9 mmol) was prepared as previously described[60] and added to a flame-dried 50 mL, 2-neck, round-bottom flask equipped with a reflux

condenser and under Ar (g). To this was added methyl-(2S)-glycidate (660 mg, 3.9 mmol), triethylamine (0.54 mL, 3.9 mmol) and 20 mL of MeOH. The mixture was stirred for 5 hours at reflux until completion of the reaction as determined by TLC. After cooling to room temperature, the mixture was concentrated *in vacuo,* and the resulting yellow oil was purified by flash column chromatography on silica gel (25% EtOAc in hexanes) to afford HO-Cys(SNB)-OMe in 35% yield (370 mg, 1.4 mmol). R_f = 0.44 (50% EtOAc in hexanes); ^{1}H NMR (300 MHz, $CDCl_3$, 298 K) δ 7.98 (1H, d, *J* = 8.2 Hz), 7.39–7.59 (3H, m), 4.44 (1H, b), 4.19 (2H, s), 3.79 (3H, s), 3.15 (1H, b), 2.89 (1H, dd, *J* = 14.4, 4.7 Hz), 2.75 (1H, dd, *J* = 14.4, 6.4 Hz); ^{13}C NMR (75 MHz, $CDCl_3$, 298K) δ 173.5, 148.6, 133.8, 133.0, 132.2, 128.3, 125.5, 71.2, 52.9, 35.3, 34.1; High-resolution MS analysis (FAB+) *m/z*: calc'd 272.0593, found 272.0591.

HO-Cys(SNB)-OMe (44 mg, 1.6 mmol) was added to a 20 mL scintillation vial and dissolved in 10 mL of 1M LiOH in 3:1:1 tetrahydrofuran: methanol: water. The mixture was stirred for 12 hours at room temperature. The pH of the solution was adjusted to pH 12 via the addition of 2 M NaOH. The aqueous layer was washed with 30 mL of ether and the organic layer was discarded. The pH of the aqueous layer was decreased to 1 via the addition of 6 M HCl, and extracted with EtOAc. The new organic layer was washed with brine, dried over Na_2SO_4 and concentrated to yield HO-Cys(SNB)-OH as a yellow oil in 85% crude yield (350 mg, 1.4 mmol). Cyanomethyl esterification began with the addition of HO-Cys(SNB)-OH (250 mg, 0.97 mmol) to a 4 mL scintillation vial. Chloroacetonitrile (0.5 mL, 7.9 mmol) and triethylamine (0.40 mL, 2.9 mmol) were added to the vial and the mixture stirred for 12 hours. The solution was diluted with 15 mL of water, and the organic layer was extracted with CH_2Cl_2 (×3), dried over Na_2SO_4

and concentrated to a yellow oil. The oil was purified by flash column chromatography on silica gel (50% EtOAC in hexanes) to afford HO-Cys(SNB)-OCH_2CN as a yellow oil in 55% yield (160 mg, 0.53 mmol). R_f = 0.35 (50% EtOAc in hexanes); ^{1}H NMR (400 MHz, $CDCl_3$, 298 K) δ 7.95 (1H, d), 7.39–7.57 (3H, m), 4.78 (2H, m), 4.52 (1H, m), 4.16 (2H, dd, *J* = 19.2, 13.3 Hz), 3.26 (1H, d, *J* = 5.5 Hz), 2.91 (1H, dd, *J* = 14.5, 3.9 Hz), 2.78 (1H, dd, *J* = 14.6, 5.9 Hz); ^{13}C NMR (100 MHz, $CDCl_3$, 298K) δ 171.4, 148.6, 133.4, 133.2, 132.2, 128.5, 125.5, 113.8, 71.0, 49.3, 35.1, 34.2; High-resolution MS analysis (FAB+) *m/z*: calc'd 297.0545, found 297.0546.

Nonsense suppression experiments. Conventional and unnatural mutagenesis were performed on mouse muscle embryonic nAChR ($\alpha1_2\beta1\gamma\delta$) cDNA in the pAMV vector using the standard Stratagene QuickChange protocol. For unnatural mutagenesis, a stop codon, TAG or TGA, was made at the site of interest and verified through sequencing. The β1 subunit contained a background mutation in the M2 transmembrane helix (β1L9'S) that is known to lower whole-cell EC_{50} values.[37, 38] The α1 subunit also contains a hemagglutinin epitope in the M3-M4 cytoplasmic loop. This epitope does not alter EC_{50} values in control experiments. cDNA was linearized with the restriction enzyme NotI. mRNA was prepared by *in vitro* transcription using the mMessage Machine T7 kit (Ambion).

Stage V-VI *Xenopus laevis* oocytes were injected with mRNA in a 2:1:1:1 or 10:1:1:1 ratio of α1:β1:γ:δ for conventional or unnatural amino acid mutagenesis experiments, respectively. Hydroxy or amino acids were appended to the dinucleotide dCA and enzymatically ligated to the truncated 74-nucleotide THG73 or TQOpS' tRNA as

previously described.[57] NVOC and 2-nitrobenzyl protecting groups on the appended amino or α-hydroxy acids were removed by irradiation with UV light filtered to ~350 nm. For conventional experiments, 1-2 ng of mRNA was injected per oocyte in a single 75 nL injection. For unnatural amino acid experiments, each cell was injected with 75 nL of a 1:1 mixture of mRNA (20-25 ng of total mRNA) and tRNA (20-30 ng). Oocytes were incubated at 18 °C for 24 to 48 hours after injection. Wild-type recovery experiments (injection of tRNA appended to the natural amino acid) were preformed to evaluate the fidelity of the unnatural suppression experiments. Additional controls, injections of mRNA only and mRNA with 76-mer THG73 or TQOpS', were also performed. While currents were seen for 76-mer control experiments, EC_{50} and Hill values were distinct from the values obtained for 74-mer ligated to an α-hydroxy or amino acid. Conventional experiments with α4β2,[33] α4β4 and α7[34] were performed as described previously.

Electrophysiology. The functional effects of mutation were evaluated using two-electrode voltage clamp electrophysiology. Electrophysiology experiments were performed 24-48 hrs after injection using the OpusXpress 6000A instrument (Axon Instruments) at a holding potential of −60 mV. A Ca^{2+} free ND96 solution was used as the running buffer (96 mM NaCl, 2 mM KCl, 1 mM $MgCl_2$, and 5 mM HEPES, pH 7.5). Acetylcholine doses in Ca^{2+}-free ND96 were applied for 15 s followed by a 116 s wash with the running buffer. Dose-response data were obtained for ≥8 agonist concentrations on ≥7 cells. All EC_{50} and Hill coefficient values were obtained by fitting dose-response relations to the Hill equation and are reported as averages ± standard error of the fit. A detailed error analysis of nonsense suppression experiments shows that data are reproducible to ±50% in EC_{50}.[61]

***Ab initio* calculations.** Structure building and subsequent *ab initio* calculations on CH_3CO-[Cys-Cys]-NH_2 were carried out using the Gaussian 03 software package[62] by Kristin Rule Gleitsman[63] at the B3LYP/6-31++G(d,p) level of theory in the gas phase. The *cis* and *trans* isomers of a model peptide of the form CH_3CO-[Cys-Cys]-NH_2 with the S-S disulfide torsional angles of ±90 were constructed using GausView molecule building tools. The geometric parameters for these starting structures were derived from the lowest energy conformers from previous *ab initio* calculations on a similar model peptide.[21] Energy minimizations were performed on the four starting structures of the model peptide. The lowest energy structures from these model peptide calculations then served as scaffolds for constructing the initial ester and *N*-methyl structures, which were subsequently subject to energy minimization calculations. In total, the energies for twelve geometry-optimized structures were calculated, with four conformers for each model system. Further details are provided in Kristin Rule Gleitsman's thesis.[63] Calculations on simple cyclic amides and related structures were performed with SPARTAN.[64]

5.6 ACKNOWLEDGEMENTS

This work was supported by the National Institutes of Health Grants NS 34407 and NS 11756.

5.7 REFERENCES

1. Corringer, P. J.; Le Novere, N.; Changeux, J. P., Nicotinic receptors at the amino acid level. *Annu. Rev. Pharmacol. Toxicol.* **2000,** 40, 431-58.
2. Grutter, T.; Changeux, J. P., Nicotinic receptors in wonderland. *Trends Biochem. Sci.* **2001,** 26, (8), 459-63.
3. Karlin, A., Emerging structure of the nicotinic acetylcholine receptors. *Nat. Rev. Neurosci.* **2002,** 3, (2), 102-14.
4. Jensen, A. A.; Frolund, B.; Liljefors, T.; Krogsgaard-Larsen, P., Neuronal nicotinic acetylcholine receptors: structural revelations, target identifications, and therapeutic inspirations. *J. Med. Chem.* **2005,** 48, (15), 4705-45.
5. Romanelli, M. N.; Gratteri, P.; Guandalini, L.; Martini, E.; Bonaccini, C.; Gualtieri, F., Central nicotinic receptors: structure, function, ligands, and therapeutic potential. *ChemMedChem* **2007,** 2, (6), 746-67.
6. Karlin, A.; Bartels, E., Effects of blocking sulfhydryl groups and of reducing disulfide bonds on the acetylcholine-activated permeability system of the electroplax. *Biochim. Biophys. Acta* **1966,** 126, (3), 525-35.
7. Karlin, A., Chemical modification of the active site of the acetylcholine receptor. *J. Gen. Physiol.* **1969,** 54, (1), 245-64.
8. Silman, I.; Karlin, A., Acetylcholine receptor: covalent attachment of depolarizing groups at the active site. *Science* **1969,** 164, (3886), 1420-1421.
9. Kao, P. N.; Dwork, A. J.; Kaldany, R. R.; Silver, M. L.; Wideman, J.; Stein, S.; Karlin, A., Identification of the alpha subunit half-cystine specifically labeled by an affinity reagent for the acetylcholine receptor binding site. *J. Biol. Chem.* **1984,** 259, (19), 11662-5.
10. Kao, P. N.; Karlin, A., Acetylcholine receptor binding site contains a disulfide cross-link between adjacent half-cystinyl residues. *J. Biol. Chem.* **1986,** 261, (18), 8085-8.
11. Czajkowski, C.; Karlin, A., Agonist binding site of *Torpedo* electric tissue nicotinic acetylcholine receptor. A negatively charged region of the delta subunit within 0.9 nm of the alpha subunit binding site disulfide. *J. Biol. Chem.* **1991,** 266, (33), 22603-22612.
12. Czajkowski, C.; Kaufmann, C.; Karlin, A., Negatively charged amino acid residues in the nicotinic receptor delta subunit that contribute to the binding of acetylcholine. *Proc. Natl. Acad. Sci. USA* **1993,** 90, (13), 6285-9.
13. Damle, V. N.; Karlin, A., Effects of agonists and antagonists on the reactivity of the binding site disulfide in acetylcholine receptor from *Torpedo californica*. *Biochemistry* **1980,** 19, (17), 3924-32.
14. Martin, M.; Czajkowski, C.; Karlin, A., The contributions of aspartyl residues in the acetylcholine receptor gamma and delta subunits to the binding of agonists and competitive antagonists. *J. Biol. Chem.* **1996,** 271, (23), 13497-503.
15. Walker, J. W.; Lukas, R. J.; McNamee, M. G., Effects of thio-group modifications on the ion permeability control and ligand binding properties of *Torpedo californica* acetylcholine receptor. *Biochemistry* **1981,** 20, (8), 2191-9.
16. Chabala, L. D.; Lester, H. A., Activation of acetylcholine receptor channels by covalently bound agonists in cultured rat myoballs. *J. Physiol.* **1986,** 379, 83-108.

17. Mishina, M.; Tobimatsu, T.; Imoto, K.; Tanaka, K.-i.; Fujita, Y.; Fukuda, K.; Kurasaki, M.; Takahashi, H.; Morimoto, Y.; Hirose, T.; Inayama, S.; Takahashi, T.; Kuno, M.; Numa, S., Location of functional regions of acetylcholine receptor alpha-subunit by site-directed mutagenesis. *Nature* **1985,** 313, (6001), 364-369.
18. Avizonis, D. Z.; Farr-Jones, S.; Kosen, P. A.; Basus, V. J., Conformations and dynamics of the essential cysteinyl-cysteine ring derived from the acetylcholine receptor. *J. Am. Chem. Soc.* **1996,** 118, (51), 13031-13039.
19. Creighton, C. J.; Reynolds, C. H.; Lee, D. H.; Leo, G. C.; Reitz, A. B., Conformational analysis of the eight-membered ring of the oxidized cysteinyl-cysteine unit implicated in nicotinic acetylcholine receptor ligand recognition. *J. Am. Chem. Soc.* **2001,** 123, (50), 12664-9.
20. Gao, F.; Mer, G.; Tonelli, M.; Hansen, S. B.; Burghardt, T. P.; Taylor, P.; Sine, S. M., Solution NMR of acetylcholine binding protein reveals agonist-mediated conformational change of the C-loop. *Mol. Pharmacol.* **2006,** 70, (4), 1230-5.
21. Hudaky, I.; Gaspari, Z.; Carugo, O.; Cemazar, M.; Pongor, S.; Perczel, A., Vicinal disulfide bridge conformers by experimental methods and by ab initio and DFT molecular computations. *Proteins* **2004,** 55, (1), 152-68.
22. Ruggles, E. L.; Deker, P. B.; Hondal, R. J., Synthesis, redox properties, and conformational analysis of vicinal disulfide ring mimics. *Tetrahedron* **2009,** 65, (7), 1257-1267.
23. Brejc, K.; van Dijk, W. J.; Klaassen, R. V.; Schuurmans, M.; van Der Oost, J.; Smit, A. B.; Sixma, T. K., Crystal structure of an ACh-binding protein reveals the ligand-binding domain of nicotinic receptors. *Nature* **2001,** 411, (6835), 269-76.
24. Celie, P. H.; van Rossum-Fikkert, S. E.; van Dijk, W. J.; Brejc, K.; Smit, A. B.; Sixma, T. K., Nicotine and carbamylcholine binding to nicotinic acetylcholine receptors as studied in AChBP crystal structures. *Neuron* **2004,** 41, (6), 907-914.
25. Capasso, S.; Mattia, C.; Mazzarella, L.; Puliti, R., Structure of a *cis*-peptide unit - molecular-conformation of cyclic disulfide *L*-cysteinyl-*L*-cysteine. *Acta Crystallogr. Sect. B-Struct. Commun.* **1977,** 33, 2080-2083.
26. Hata, Y.; Matsuura, Y.; Tanaka, N.; Ashida, T.; Kakudo, M., Tert-butyloxycarbonyl-*L*-cysteinyl-*L*-cysteine disulfide methyl-ester. *Acta Crystallogr. Sect. B-Struct. Commun.* **1977,** 33, 3561-3564.
27. Grosman, C.; Zhou, M.; Auerbach, A., Mapping the conformational wave of acetylcholine receptor channel gating. *Nature* **2000,** 403, (6771), 773-6.
28. Dugave, C.; Demange, L., *Cis-trans* isomerization of organic molecules and biomolecules: Implications and applications. *Chem. Rev.* **2003,** 103, (7), 2475-2532.
29. Aubry, A.; Vitoux, B.; Boussard, G.; Marraud, M., *N*-Methyl peptides. IV. Water and beta-turn in peptides. Crystal structure of *N*-pivaloyl-*L*-prolyl-*N*,*N*′-dimethyl-*D*-alaninamide in the anhydrous and monohydrated states. *Int. J. Pept. Protein Res.* **1981,** 18, (2), 195-202.
30. Vitoux, B.; Aubry, A.; Cung, M. T.; Boussard, G.; Marraud, M., *N*-methyl peptides. III. Solution conformational study and crystal structure of *N*-pivaloyl-*L*-prolyl-*N*-methyl-*N*′-isopropyl-*L*-alaninamide. *Int. J. Pept. Protein Res.* **1981,** 17, (4), 469-79.

31. Beene, D. L.; Dougherty, D. A.; Lester, H. A., Unnatural amino acid mutagenesis in mapping ion channel function. *Curr. Opin. Neurobiol.* **2003,** 13, (3), 264-70.
32. Nowak, M. W.; Kearney, P. C.; Sampson, J. R.; Saks, M. E.; Labarca, C. G.; Silverman, S. K.; Zhong, W.; Thorson, J.; Abelson, J. N.; Davidson, N.; Schultz, P. G.; Dougherty, D. A.; Lester, H. A., Nicotinic receptor binding site probed with unnatural amino acid incorporation in intact cells. *Science* **1995,** 268, 439-442.
33. Xiu, X.; Puskar, N. L.; Shanata, J. A.; Lester, H. A.; Dougherty, D. A., Nicotine binding to brain receptors requires a strong cation-pi interaction. *Nature* **2009,** 458, (7237), 534-7.
34. Puskar, N. L.; Xiu, X.; Lester, H. A.; Dougherty, D. A., Two neuronal nicotinic acetylcholine receptors, alpha4beta4 and alpha7, show differential agonist binding modes. *J. Biol. Chem.* **2011,** 286, (16), 14618-27.
35. Horovitz, A., Double-mutant cycles: a powerful tool for analyzing protein structure and function. *Fold. Des.* **1996,** 1, (6), R121-6.
36. Makhatadze, G. I.; Loladze, V. V.; Ermolenko, D. N.; Chen, X. F.; Thomas, S. T., Contribution of surface salt bridges to protein stability: Guidelines for protein engineering. *J. Mol. Biol.* **2003,** 327, (5), 1135-1148.
37. Filatov, G. N.; White, M. M., The role of conserved leucines in the M2 domain of the acetylcholine receptor in channel gating. *Mol. Pharmacol.* **1995,** 48, (3), 379-84.
38. Labarca, C.; Nowak, M. W.; Zhang, H.; Tang, L.; Deshpande, P.; Lester, H. A., Channel gating governed symmetrically by conserved leucine residues in the M2 domain of nicotinic receptors. *Nature* **1995,** 376, 514-516.
39. Gleitsman, K. R.; Kedrowski, S. M. A.; Lester, H. A.; Dougherty, D. A., An intersubunit hydrogen bond in the nicotinic acetylcholine receptor that contributes to channel gating. *J. Biol. Chem.* **2008,** 283, (51), 35638-35643.
40. Beligere, G. S.; Dawson, P. E., Design, synthesis, and characterization of 4-ester C12, a model for backbone hydrogen bonding in protein α-helices. *J. Am. Chem. Soc.* **2000,** 122, (49), 12079-12082.
41. Blankenship, J. W.; Balambika, R.; Dawson, P. E., Probing backbone hydrogen bonds in the hydrophobic core of GCN4. *Biochemistry* **2002,** 41, (52), 15676-84.
42. Deechongkit, S.; Dawson, P. E.; Kelly, J. W., Toward assessing the position-dependent contributions of backbone hydrogen bonding to beta-sheet folding thermodynamics employing amide-to-ester perturbations. *J. Am. Chem. Soc.* **2004,** 126, (51), 16762-71.
43. Deechongkit, S.; Nguyen, H.; Powers, E. T.; Dawson, P. E.; Gruebele, M.; Kelly, J. W., Context-dependent contributions of backbone hydrogen bonding to beta-sheet folding energetics. *Nature* **2004,** 430, (6995), 101-5.
44. Koh, J. T.; Cornish, V. W.; Schultz, P. G., An experimental approach to evaluating the role of backbone interactions in proteins using unnatural amino acid mutagenesis. *Biochemistry* **1997,** 36, (38), 11314-22.
45. Nakhle, B. M.; Silinski, P.; Fitzgerald, M. C., Identification of an essential backbone amide bond in the folding and stability of a multimeric enzyme. *J. Am. Chem. Soc.* **2000,** 122, (34), 8105-8111.

46. Horovitz, A.; Serrano, L.; Avron, B.; Bycroft, M.; Fersht, A. R., Strength and co-operativity of contributions of surface salt bridges to protein stability. *J. Mol. Biol.* **1990,** 216, (4), 1031-44.
47. Marqusee, S.; Sauer, R. T., Contributions of a hydrogen bond/salt bridge network to the stability of secondary and tertiary structure in lambda repressor. *Protein Sci.* **1994,** 3, (12), 2217-25.
48. Waldburger, C. D.; Schildbach, J. F.; Sauer, R. T., Are buried salt bridges important for protein stability and conformational specificity? *Nat. Struct. Biol.* **1995,** 2, (2), 122-8.
49. Miyazawa, A.; Fujiyoshi, Y.; Stowell, M.; Unwin, N., Nicotinic acetylcholine receptor at 4.6 Å resolution: transverse tunnels in the channel wall. *J. Mol. Biol.* **1999,** 288, (4), 765-86.
50. Unwin, N., Refined structure of the nicotinic acetylcholine receptor at 4Å resolution. *J. Mol. Biol.* **2005,** 346, (4), 967-89.
51. Blum, A. P.; Gleitsman, K. R.; Lester, H. A.; Dougherty, D. A., Evidence for an extended hydrogen bond network in the binding site of the nicotinic receptor: concerning the role of the vicinal disulfide of the α1 subunit. *J. Biol. Chem.* **2011**, 286, (37), 32251-58.
52. Czajkowski, C.; Karlin, A., Structure of the nicotinic receptor acetylcholine-binding site. *J. Biol. Chem.* **1995,** 270, (7), 3160-64.
53. Zhong, W.; Gallivan, J. P.; Zhang, Y.; Li, L.; Lester, H. A.; Dougherty, D. A., From *ab initio* quantum mechanics to molecular neurobiology: a cation-pi binding site in the nicotinic receptor. *Proc. Natl. Acad. Sci. USA* **1998,** 95, (21), 12088-93.
54. Akk, G.; Zhou, M.; Auerbach, A., A mutational analysis of the acetylcholine receptor channel transmitter binding site. *Biophys J.* **1999,** 76, 207-18.
55. Sine, S. M.; Shen, X. M.; Wang, H. L.; Ohno, K.; Lee, W. Y.; Tsujino, A.; Brengmann, J.; Bren, N.; Vajsar, J.; Engel, A. G., Naturally occurring mutations at the acetylcholine receptor binding site independently alter ACh binding and channel gating. *J. Gen. Physiol.* **2002,** 120, (4), 483-96.
56. Silverman, S. K., I. Conformational and charge effects on high-spin organic polyradicals. II. Studies on the atomic-scale basis of ion selectivity in potassium channels. Ph.D. Thesis. California Institute of Technology, Pasadena, CA, 1998.
57. Nowak, M. W.; Gallivan, J. P.; Silverman, S. K.; Labarca, C. G.; Dougherty, D. A.; Lester, H. A., [28] *In vivo* incorporation of unnatural amino acids into ion channels in Xenopus oocyte expression system. In *Methods in Enzymology*, Conn, P. M., Ed. Academic Press: 1998; Vol. Volume 293, pp 504-529.
58. Park, J. D.; Kim, D. H., Cysteine derivatives as inhibitors for carboxypeptidase a: synthesis and structure-activity relationships. *J. Med. Chem.* **2002,** 45, (4), 911-918.
59. Deechongkit, S.; You, S.-L.; Kelly, J. W., Synthesis of all nineteen appropriately protected chiral α-hydroxy acid equivalents of the α-amino acids for boc solid-phase depsi-peptide synthesis. *Org. Lett.* **2004,** 6, (4), 497-500.
60. Sohn, C. H.; Chung, C. K.; Yin, S.; Ramachandran, P.; Loo, J. A.; Beauchamp, J. L., Probing the mechanism of electron capture and electron transfer dissociation using tags with variable electron affinity. *J. Amer. Chem. Soc.* **2009,** 131, (15), 5444-5459.

61. Torrice, M. M. Chemical-scale studies of the nicotinic and muscarinic acetylcholine receptors. Ph.D. Thesis. California Insitute of Technology, Pasadena, CA, 2009.
62. Frisch, M. J.; Trucks, G. W.; Schlegel, H. B.; Scuseria, G. E.; Robb, M. A.; Cheeseman, J. R.; Montgomery, J. A.; Vreven, T.; Kudin, K. N.; Burant, J. C.; Millam, J. M.; Iyengar, S. S.; Tomasi, J.; Barone, V.; Mennucci, B.; Cossi, M.; Scalmani, G.; Rega, N.; Petersson, G. A.; Nakatsuji, H.; Hada, M.; Ehara, M.; Toyota, K.; Fukuda, R.; Hasegawa, J.; Ishida, M.; Nakajima, T.; Honda, Y.; Kitao, O.; Nakai, H.; Klene, M.; Li, X.; Knox, J. E.; Hratchian, H. P.; Cross, J. B.; Bakken, V.; Adamo, C.; Jaramillo, J.; Gomperts, R.; Stratmann, R. E.; Yazyev, O.; Austin, A. J.; Cammi, R.; Pomelli, C.; Ochterski, J. W.; Ayala, P. Y.; Morokuma, K.; Voth, G. A.; Salvador, P.; Dannenberg, J. J.; Zakrzewski, V. G.; Dapprich, S.; Daniels, A. D.; Strain, M. C.; Farkas, O.; Malick, D. K.; Rabuck, A. D.; Raghavachari, K.; Foresman, J. B.; Ortiz, J. V.; Cui, Q.; Baboul, A. G.; Clifford, S.; Cioslowski, J.; Stefanov, B. B.; Liu, G.; Liashenko, A.; Piskorz, P.; Komaromi, I.; Martin, R. L.; Fox, D. J.; Keith, T.; Laham, A.; Peng, C. Y.; Nanayakkara, A.; Challacombe, M.; Gill, P. M. W.; Johnson, B.; Chen, W.; Wong, M. W.; Gonzalez, C.; Pople, J. A., Gaussian 03, Revision C.02. In 2003.
63. Gleitsman, K. R., Chemical-scale studies of the nicotinic acetylcholine receptor: insights from amide-to-ester backbone mutagenesis. Ph.D. Thesis. California Institute of Technology, Pasadena, CA **2010**.
64. SPARTAN, *Wavefunction, Inc. Irvine, CA*.